Journal of
Plant Ecology

Research article

Marine heatwaves intensify competition between toxigenic microalgae and cultured macroalgae

Yonglong Xiong[1,2], Jingke Ge[1], Fei-Xue Fu[3], David A. Hutchins[3], Lixue Luo[1], Jiaying Wen[1] AQ2 AQ1 and Guang Gao[1,2,*]

[1]State Key Laboratory of Marine Environmental Science & College of Ocean and Earth Sciences, Xiamen University, Xiamen 361005, China, [2]Ocean Decade International Cooperation Center, Qingdao 266000, China, [3]Marine and Environmental Biology, University of Southern AQ3 California, Los Angeles, CA, USA

[*]Corresponding author. E-mail: guang.gao@xmu.edu.cn

Handling Editor: Qiang* He

Received: 12 March 2026, **First Decision:** 10 April 2026, **Accepted:** 30 April 2026

Citation: Xiong Yonglong, Ge Jingke, Fu Fei-Xue, Hutchins David A., Luo Lixue, Wen Jiaying, Gao Guang (2026) Marine heatwaves intensify competition between toxigenic microalgae and cultured macroalgae. *J Plant Ecol* **00**:rtag108. https://doi.org/10.1093/jpe/rtag108

Abstract

Harmful algal blooms (HABs) and marine heatwaves (MHWs) are occurring with increasing frequency, posing significant threats to marine ecosystems. Macroalgae cultivation has been demonstrated to inhibit the occurrence of HABs. However, how MHWs affect the interactive dynamics between toxigenic microalgae and cultivated macroalgae remains poorly understood. In this study, an economically important macroalga *Gracilariopsis lemaneiformis* and a globally distributed bloom-forming toxigenic microalga *Heterosigma akashiwo* were grown in monoculture and coculture systems under a simulated MHW event to bridge this gap. Co-culture with *G. lemaneiformis* significantly reduced the relative growth rate of *H. akashiwo*. This inhibitory effect could be attributed to allelochemicals secreted by *G. lemaneiformis*, which decreased the photosynthetic efficiency (Fv/Fm) of the microalga. Notably, heatwave conditions exacerbated these inhibitory effects, and *H. akashiwo* showed no signs of recovery even after the post-heatwave recovery period. In the co-culture system, increased microalgal toxicity reduced the phycobiliprotein content in *G. lemaneiformis*. Despite increased metabolic activity in the macroalga, its overall relative growth rates ultimately decreased, with heatwaves exacerbating this reduction. Metabolomic analysis revealed that both the heatwave and co-cultivation with toxic microalgae significantly disrupted the metabolic homeostasis of *G. lemaneiformis*, particularly its carbon and nitrogen, lipid and nucleotide metabolisms, ultimately forcing the macroalgae to reallocate energy resources toward essential survival functions. These findings indicate that MHWs could intensify competition between *H. akashiwo* and *G. lemaneiformis,* providing novel insights into the potential ecological risks posed by toxigenic microalgae and MHWs to aquaculture.

Keywords: harmful algal bloom, interspecific competition, marine heatwave, metabolomics, seaweed aquaculture, toxicity

© The Author(s) 2026. Published by Oxford University Press on behalf of Institute of the Botany, Chinese Academy of Sciences and the Botanical Society of China.
This is an Open Access article distributed under the terms of the Creative Commons Attribution License (https://creativecommons.org/licenses/by/4.0/), which permits unrestricted reuse, distribution, and reproduction in any medium, provided the original work is properly cited.

海洋热浪加剧产毒微藻与养殖大型海藻间的竞争

摘要

有害藻华（HABs）与海洋热浪（MHWs）的发生频率日益增加，对海洋生态系统构成重大威胁。研究表明，大型海藻养殖能抑制有害藻华的发生，然而，目前对于海洋热浪如何影响产毒微藻与养殖大型海藻之间的相互作用尚不清楚。本研究以经济大型海藻龙须菜（*Gracilariopsis lemaneiformis*）和全球分布的产毒微藻赤潮异弯藻（*Heterosigma akashiwo*）为研究对象，在模拟海洋热浪的条件下，分别进行单培养和共培养实验，以探讨两者的相互作用关系。结果显示，与龙须菜共培养显著降低了赤潮异弯藻的相对生长率。这种抑制作用可能源于龙须菜分泌的化感物质对微藻光合效率（Fv/Fm）的抑制效应。值得注意的是，热浪条件进一步强化了这种抑制作用，且即便在热浪后的恢复期内，赤潮异弯藻亦未显示出恢复迹象。在共培养体系中，微藻毒性的增加降低了龙须菜体内藻胆蛋白含量; 尽管大型海藻的代谢活性有所增强，但其总体相对生长率仍然下降，而热浪进一步加剧了这种下降。代谢组学分析显示，无论是热浪还是与有毒微藻共培养，均显著扰乱了龙须菜的代谢稳态，特别是碳氮代谢、脂质代谢及核苷酸代谢，迫使大型海藻将能量重新分配至维持基础生存的关键功能。这些发现表明，海洋热浪会加剧赤潮异弯藻与龙须菜之间的竞争，为有毒微藻和海洋热浪对水产养殖构成的潜在生态风险提供了新的认知。

关键词：有害藻华，种间竞争，海洋热浪，代谢组学，海藻养殖，毒性

AQ4

INTRODUCTION

Harmful algal blooms (HABs) have emerged as a critical environmental problem in coastal waters worldwide in recent decades (Dai *et al.* 2023). In particular, HABs caused by toxigenic microalgae pose detrimental effects on aquaculture, marine ecosystems and human health (Hallegraeff *et al.* 2021). Algal toxin production results not only in mass mortality of fish in coastal areas (Mardones *et al.* 2023) but also negative impacts on the physiology and growth of macroalgae (Pflugmacher *et al.* 2010; Wu *et al.* 2025b). More alarmingly, these algal toxins can bioaccumulate through the food web, ultimately posing substantial health risks to humans (Li *et al.* 2021). These environmental impacts escalate during the decay phase of algal blooms by depleting dissolved oxygen and releasing toxic substances, thereby accelerating environmental deterioration and potentially triggering ecosystem collapse (O'Boyle *et al.* 2016; Wang *et al.* 2021).

Macroalgae play a vital role in aquatic environments as important primary producers and make substantial contributions to the marine economy (García-Poza *et al.* 2022). The scale of macroalgae cultivation is continuously expanding (Xiong *et al.* 2023), and they also demonstrate tremendous potential for carbon sequestration (Gao *et al.* 2022; Li *et al.* 2022). In addition, accumulating evidence suggests that macroalgae employ diverse mechanisms to effectively suppress HABs. For instance, macroalgae directly compete with red tide microalgae for nutrients, thereby limiting the proliferation of HABs (Sylvers and Gobler 2021). In addition, macroalgae can produce and release various bioactive allelopathic compounds into the surrounding environment. These compounds not only can inhibit HAB growth and reproduction (Accoroni *et al.* 2015; Gao *et al.* 2019) but also can enhance overall phytoplankton biodiversity by preventing the dominance of particular species, thereby promoting the stability of coastal ecosystems (Chai *et al.* 2018).

Marine heatwaves (MHWs) are defined as prolonged periods of anomalously warm ocean waters (Hobday *et al.* 2016) and cause significant threats to marine ecosystems (Frolicher and Laufkotter 2018). Over recent decades, MHWs have been documented globally with increasing frequency, duration and intensity, primarily driven by continuous greenhouse gas emissions (Laufkötter *et al.* 2020; Oliver *et al.* 2018). The ecological impacts of MHWs are complex and multifaceted. The response of HABs to MHWs varies with nutrient availability: in nutrient-poor waters, MHWs are associated with weaker HABs development, whereas in nutrient-rich waters, they can promote more intense bloom events (Hayashida *et al.* 2020). A MHW event, which promoted blooms

of the diatom *Chaetoceros coarctatus*, led to widespread mortalities of marine organisms (Roberts *et al.* 2019). Furthermore, MHWs may initially facilitate the bloom formation of the harmful dinoflagellate *Cochlodinium polykrikoides*, but ultimately have negative effects on bloom maintenance (Lim *et al.* 2021). A multi-year heatwave in the North Pacific Ocean produced the most toxic, most persistent and most widespread bloom of the HAB diatom *Pseudonitzschia* spp. ever recorded (McCabe *et al.* 2016; Zhu *et al.* 2017). Beyond its effects on phytoplankton communities, MHWs significantly impact the growth and survival of macroalgae. MHWs can disrupt the physiological metabolism of macroalgae along the coastal waters of China, inhibiting their growth and increasing the risk of decay and mortality (Gao *et al.* 2024; Jiang *et al.* 2022; Sheng *et al.* 2025). At broader scales, MHWs reduce the productivity of macroalgal forests and alter their carbon budgets in the Mediterranean Sea (Bulleri *et al.* 2025) and can also drive large-scale shifts in kelp forest structure along the coast of California, with cascading impacts on ecosystem functioning (McPherson *et al.* 2021).

Heterosigma akashiwo (Raphidophyceae) is a globally distributed harmful microalga that produces ichthyotoxins, causing substantial economic losses in aquaculture due to fish mortality (Mardones *et al.* 2023). *H. akashiwo* has also been shown to benefit more from warming relative to some other microalgae (Fu *et al.* 2008). The macroalga *Gracilariopsis lemaneiformis* (Gracilariaceae, Rhodophyta) is an economically important marine crop, as it exhibits the merits of robust temperature adaptability and rapid growth. Therefore, it is the most extensively farmed macroalga along the China coast (Fei 2004; Gao *et al.* 2022). Traditionally, macroalgal cultivation areas have demonstrated lower frequencies of HABs, primarily due to the natural inhibitory properties of macroalgae. However, recent evidence suggests an increasing frequency of red tide events in these areas, potentially related to global climate change (Hu *et al.* 2026). While several studies have investigated how heatwaves affect the ability of *G. lemaneiformis* to inhibit red tide microalgae (Gao *et al.* 2024; Zhao *et al.* 2025), two critical knowledge gaps remain: (i) how MHWs influence the toxicity of toxigenic microalgae and (ii) the complex interactions between toxigenic microalgae and *G. lemaneiformis* during MHWs. Blooms of *H. akashiwo* have been reported in the East China Sea where *G. lemaneiformis* is extensively cultivated (Ji *et al.* 2018; Xiong *et al.* 2023). Therefore, in the present study, *H. akashiwo* and *G. lemaneiformis* were grown in monoculture and coculture systems under simulated MHW conditions, and their physiological responses, the macroalgal metabolome and microalgal hemolytic activity were analyzed to explore the potential mechanisms underlying the evolution of their interplay.

MATERIALS AND METHODS

Algal collection and culture

The HAB raphidophyte *Heterosigma akashiwo* (CCMA369) was provided by the Center for Collections of Marine Algae at Xiamen University. It was isolated from the Yangtze Estuary in the East China Sea, a region adjacent to where *G. lemaneiformis* is cultivated (Cheng *et al.* 2024). The cultures were inoculated in 1000 mL modified f/2 without silica medium prepared with sterile natural seawater. The algal cultures were incubated at 22 °C, under a photoperiod of 12 h light: 12 h dark, with a light intensity of 100 μmol photons m^{-2} s^{-1}. Before the experiment, *H. akashiwo* was treated with Penicillin-Streptomycin solution (Procell, China) for 24 h, to reduce bacterial impacts on algae as much as possible. The final concentration was 200 U·mL^{-1} penicillin and 0.2 mg·mL^{-1} streptomycin (Gao *et al.* 2024), and the antibiotic treatment had no detectable effect on *H. akashiwo* (Supplementary Fig. S1). The medium was renewed in semi-continuous mode every 3 days before the experiment to keep the cells in the exponential growth phase.

Gracilariopsis lemaneiformis was obtained from a macroalgal culture area in Sansha Bay (119.31°E, 26.39°N), Ningde City, Fujian Province in November 2023. The sample was transported back to the laboratory under low temperature, dark conditions. The thalli were cleaned using natural seawater using 0.22 μm pore size filter. Thalli with similar branch length and thickness were selected, and other attached algae were removed by gently wiping the surfaces of thalli with degreased cotton in alcohol, and this treatment was confirmed to cause no damage to the thalli through pre-experiment (Supplementary Fig. S2a and b). *G. lemaneiformis* was also treated with antibiotics (400 U·mL^{-1} penicillin and 0.4 mg·mL^{-1} streptomycin) for 48 h, and then washed repeatedly with sterilized seawater to wash off the antibiotics (Chai *et al.* 2021; Zhao *et al.* 2025). Preliminary experiments confirmed that this antibiotic exposure caused no physiological damage

to the thalli (Supplementary Fig. S2c and d). The culture temperature, light and other conditions were consistent with those used to grow *H. akashiwo*, and the culture medium was renewed every 3 days to maintain the growth and activity of the thalli.

Experimental design

The experimental design was based on modifications of methods used in previous studies (Gao *et al.* 2024; Zhao *et al.* 2025). Co-cultures of both species together and monoculture systems of each species alone were used in the experiment (Fig. 1a). The AQ5 experimental culture containers were 1 L transparent glass conical bottles. The culture was bubbled with outdoor air filtered by 0.22 μm filter membrane. To maintain sufficient nutrient supply and reduce potential nutrient-mediated effects, 50% of the culture medium was renewed every 3 days under a semicontinuous cultivation system (Supplementary Fig. S3). Every treatment has four repetitions. The initial density of *H. akashiwo* and

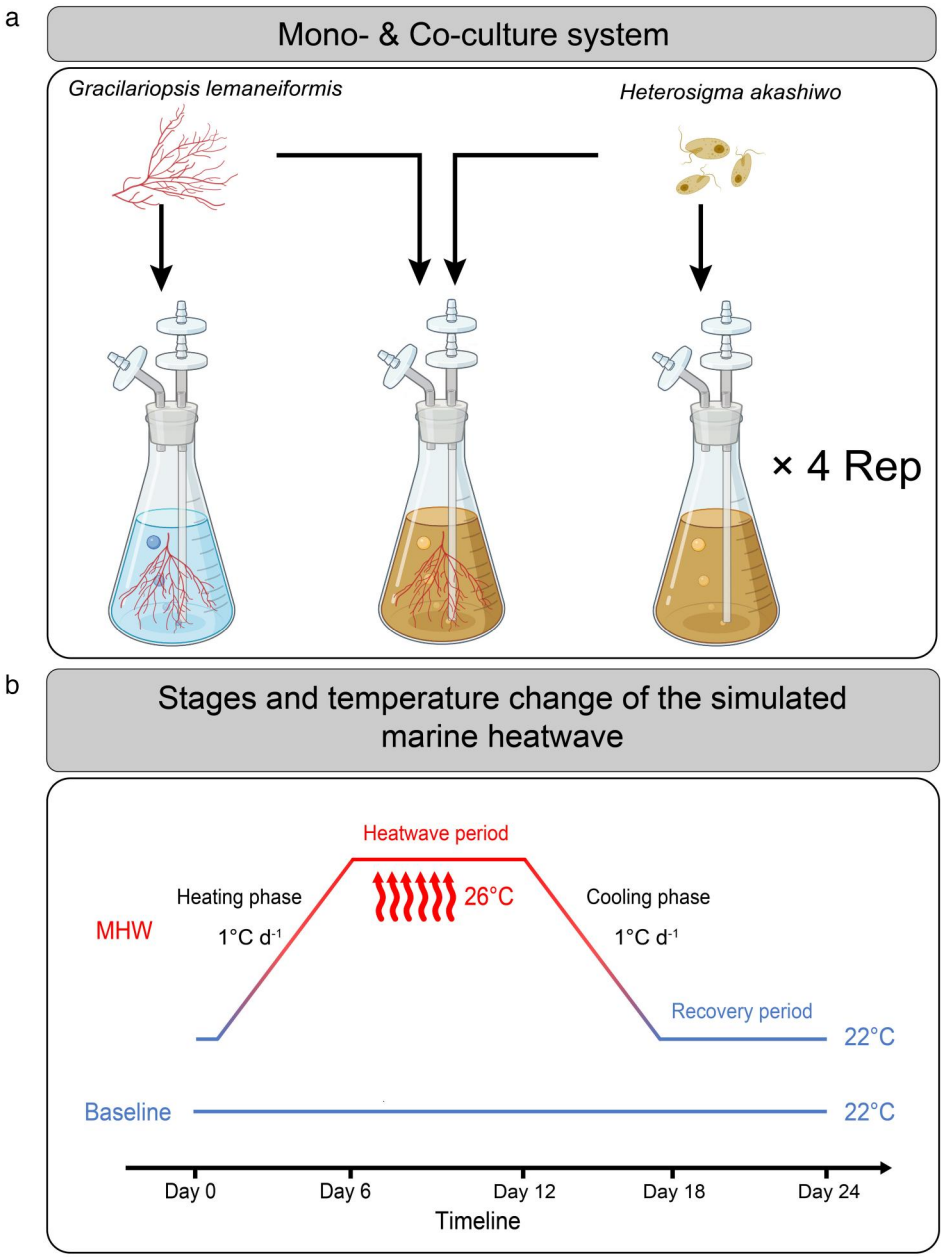

Figure 1: The experimental design of the study. (a) mono- and co-culture systems with four repetitions for each treatment. AQ20 (b) stages and temperature change of the simulated marine heatwave.

G. lemaneiformis were 1×10^4 cells mL^{-1} and 1 g L^{-1}, respectively, which represent a common density for a red tide of *H. akashiwo* (Baohong *et al.* 2021) and a typical culture density of *G. lemaneiformis* in the aquaculture area (Gao *et al.* 2024).

The experiment included the following temperature treatments: a control group (22 °C, Baseline) and a heatwave treatment group (26 °C, Heatwave). The East China Sea experiences frequent occurrences of red tides in April (spring), with mean monthly temperatures of 22 °C (Bao and Ren 2014; Li 2021). According to temperature monitoring data, a 4 °C MHW can occur in the coastal waters of China (Li *et al.* 2019). To investigate the impact of a 4 °C spring heatwave event on both red-tide microalgae and macroalgae, we simulated MHW conditions by elevating temperatures from baseline (22 °C) to 26 °C in the treatment group. The temperature design in the heatwave treatment group consisted of four sequential phases: (i) a heating phase where temperature increased from 22 °C to 26 °C at a rate of 1 °C d^{-1}, (ii) a heatwave period when temperature was kept at 26 °C for a week, (iii) a cooling phase where temperature decreased to 22 °C at a rate of 1 °C d^{-1} and (iv) a recovery period when temperature was held constant at 22 °C until the end of experiment (Fig. 1b). The experiment lasted for 24 days in total.

Determination of relative growth rate

The cell density was measured every 3 days. 15–20 mL of samples were collected for cell density measurement. The cell density was determined using a particle counter and size analyzer (Z2 Coulter, Beckman, USA). The measurement of relative growth rate of *G. lemaneiformis* was done in an ultra-clean workbench. Thalli were taken from the culture bottles, wiped with absorbent paper and their fresh weight was measured with an analytical balance (HZK-FA110, HZ, USA) calibrated to a sensitivity of 0.1 mg. The relative growth rates (RGRs) of *H. akashiwo* and *G. lemaneiformis* were calculated according to the formula:

$$\mathrm{RGR}\ (d^{-1}) = (\ln N_1 - \ln N_0)/\ (t_1 - t_0)$$

where N_1 and N_0 represent the cell concentrations of *H. akashiwo* or the fresh weight of *G. lemaneiformis* at t_1 and t_0, respectively.

Estimation of photosynthetic activity

The maximal quantum yield of PSII (Fv/Fm), the effective quantum yield of PSII (Y(II)) and non-photochemical quenching (NPQ) were determined using a Multi-color PAM (Walz, Germany) to assess the photosynthetic activity of the algae. For *H. akashiwo*, cells from different treatments were sampled in a 10 mL sterilized centrifuge tube and placed at the culture temperature for dark adaptation for 15 min to ensure that PSII reaction centers were fully open. The saturated pulse for Fv/Fm measurements was set at 4500 μmol photons m^{-2} s^{-1} (0.8 s). The measurement system employed 440-nm white light, and the actinic light intensity was maintained at identical levels to the experimental growth conditions after the saturated pulse. For *G. lemaneiformis*, the thalli were placed in a sterilized 10 mL centrifuge tube with seawater from the corresponding culture bottle. Afterward, dark adaptation and measurement processes were consistent with the previous description.

Determination of photosynthetic pigments

For *G. lemaneiformis*, approximately 0.02 g (FW) thalli were collected and extracted in 5 mL absolute methanol at 4 °C in darkness for 24 h. Before the measurement, the extract was shaken evenly, then centrifuged at 8000 rpm/min at 4 °C for 10 min by using a high-speed refrigerated centrifuge (Universal 320R, Hettich, Germany). The supernatant was taken and measured with an ultraviolet spectrophotometer (TU-1810DASPC, China) with absolute methanol as reference. For *H. akashiwo*, 10 mL of the sample was filtered on 25 mm GF/F filters (Whatman, USA) and extracted in 5 mL absolute methanol at 4 °C in darkness for 24 h. The extract was centrifuged, measured as described above.

The contents of Chl *a* and carotenoids were calculated according to the following formulas (Porra *et al.* 1989; Strickland and Parsons 1972):

$$\mathrm{Chl}\,a\,(\mu g\ mL^{-1}) = 16.29 \times (A_{665} - A_{750}) - 8.54 \times (A_{652} - A_{750})$$

$$\mathrm{Carotenoids}\ (\mu g\ mL^{-1}) = 7.6 \times (A_{480} - A_{750}) - 1.49 \times (A_{510} - A_{750})$$

To determine phycoerythrin (PE) and phycocyanin (PC) in *G. lemaneiformis*, about 0.05 g (FW) thalli were collected and disrupted by grinding with a glass homogenizer in an ice bath and extracted in 0.1 M PBS buffer (pH = 6.8). The final volume of extract was 10 mL. The extract was then centrifuged

at 9000 rpm/min at 4 °C for 10 min in a high-speed refrigerated centrifuge (Universal 320R, Hettich, Germany). The supernatant was taken and measured with an ultraviolet spectrophotometer (TU-1810DASPC, China) with PBS buffer as blank control.

The contents of PE and PC were calculated by the formulas (Beer and Eshel 1985):

$$\text{PE } (\mu g\ mL^{-1}) = [(A_{564}-A_{592})-(A_{455}-A_{592})\times 0.2]\times 0.12$$

$$\text{PC } (\mu g\ mL^{-1}) = [(A_{618}-A_{645})-(A_{592}-A_{645})\times 0.51]\times 0.15$$

where A_{750}, A_{665}, A_{652}, A_{510}, A_{480}, A_{645}, A_{618}, A_{592}, A_{564} and A_{455} are the absorbance wavelength at 750, 665, 652, 510, 480, 645, 618, 592, 564 and 455 nm, respectively. The results were expressed as pg·cell^{-1} for *H. akashiwo* and mg·g^{-1} FW for *G. lemaneiformis*.

Hemolytic activity of *H. akashiwo*

Hemolytic activity was determined according to modified protocols from Eschbach *et al.* (2001) and Ling and Trick (2010). Detailed procedures for algal sample preparation, erythrocyte handling and erythrocyte lysis assays are described in Supplementary Text S1. Hemolytic activity of each treatment was expressed as the percentage hemolysis relative to both the blank control (reagent absorption), positive control (erythrocyte complete lysis) and negative control (erythrocyte autolysis), according to the following equation:

$$\text{Hemolytic activity } (\%) = [(E_{414}-B_{414}-N_{414})/\ P_{414}]\times 100\%$$

Where E_{414}, B_{414}, N_{414} and P_{414}, are absorption of the experimental treatment, blank control, negative control and positive control, respectively. The hemolytic activity unit was converted into $\times 10^{-7}$% cell^{-1}. The values above zero were considered hemolytic, whereas the values at or below zero were considered non-hemolytic.

Metabolomic analysis of *G. lemaneiformis*

Due to the suppressed biomass of *H. akashiwo* falling below the required threshold (10^7 cells) for metabolomics, we focused the analysis on *G. lemaneiformis*. Approximately 0.1 g (FW) thalli of *G. lemaneiformis* from each culture were collected in a sterilized 2 mL cryotube on the last day of the heatwave (Day 12) and recovery period (Day 24), frozen with liquid nitrogen and stored at −80 °C (Gao *et al.* 2024). Detailed procedures for sample preparation, LC-MS detection, data preprocessing and statistical analysis were provided in Supplementary Text S2. The differentially expressed metabolites (DEMs) in different treatments were detected with variable importance in the projection >1, $P < 0.05$. The metabolic pathways of differential metabolites were annotated by the KEGG database (Gao *et al.* 2024).

Statistical analysis

The experimental data were statistically analyzed using SPSS 26 and R (version 4.4.1), and plotted by Origin 2024 and R. The generalized additive mixed models (GAMMs) were used to analyze the patterns of treatment effects over time, and GAMMs were performed using the 'mgcv' package in R. Prior to ANOVA, data were tested for normality using the Shapiro–Wilk test and for homogeneity of variances using Levene's test. The data were confirmed to have a normal distribution and the variances were equal for all treatments ($P > 0.05$). Two-way ANOVA was used to examine the effects of heatwave and co-culture on physiological traits of algae. One-way ANOVA was used to establish the significance of differences among treatments on the same day. Fisher's least significant difference of *post hoc* testing was analyzed, and the significance level was set as $P < 0.05$.

RESULTS

Growth responses of *H. akashiwo* and *G. lemaneiformis*

The RGR of *H. akashiwo* was lower in coculture than in monoculture during most of the experimental period, except for Day 21 (Supplementary Table S1). During the heatwave period, the lowest RGR values were observed in the co-heatwave treatment (Fig. 2a). On Day 9, RGR in co-baseline and co-heatwave treatments was 92% and 196% lower than that in the mono-baseline treatment, respectively ($P = 0.018$). During the recovery period (Day 21), relative to the mono-baseline treatment, RGR still decreased by 69% in the co-baseline treatment and increased by 58% in the co-heatwave treatment ($P = 0.004$). The GAMM analysis further revealed that the inhibitory effect of co-baseline

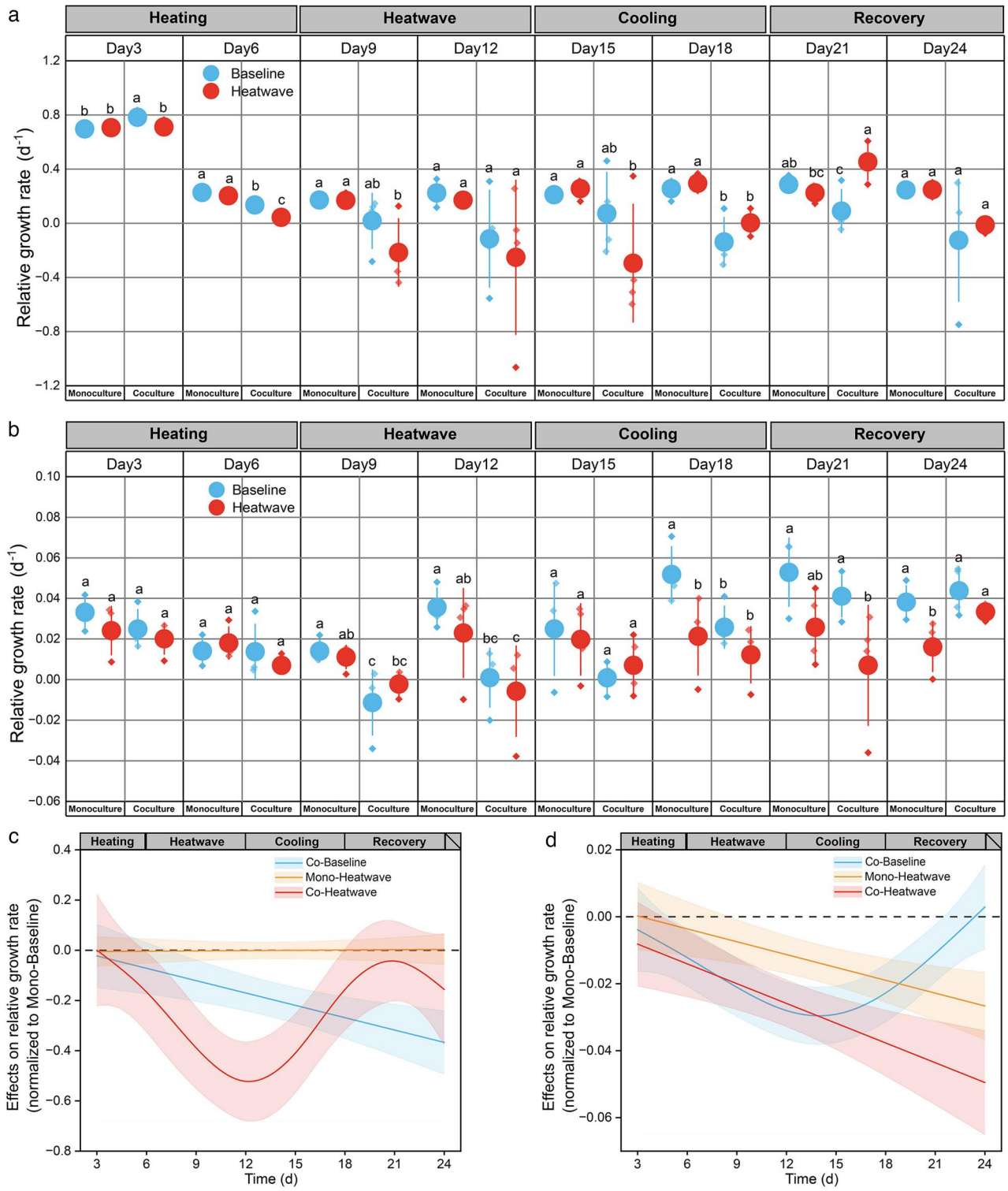

Figure 2: Growth responses of *Heterosigma akashiwo* and *Gracilaria lemaneiformis* under different treatments. The RGR of *H. akashiwo* (a) and *G. lemaneiformis* (b). Values represent mean ± standard deviation (SD), with different letters indicating statistically significant differences among treatments on the same day ($P < 0.05$). Normalized effects of treatment groups on RGR relative to the mono-control treatment based on GAMM analysis for *H. akashiwo* (c) and *G. lemaneiformis* (d). Treatments are colored with blue (co-baseline), yellow (mono-heatwave) and red (co-heatwave). Solid lines and shadows are predicted values with 95% confidence intervals, and the significant differences between the different treatment groups and the mono-baseline are justified by the lack of intersections of 95% confidence intervals and the x-axis. Heating, heatwave, cooling and recovery represent the four phases of experiment.

AQ21

treatment strengthened over time ($P = 0.004$), whereas the negative effect of the co-heatwave treatment increased during the heatwave period and weakened during the recovery period ($P = 0.008$) (Fig. 2c).

For *G. lemaneiformis*, coculture treatment markedly reduced its RGR during the heatwave period (Supplementary Table S2). Specifically, on Day 9, RGR decreased by 181% and 116% in co-baseline and co-heatwave treatments, respectively (Fig. 2b, $P = 0.008$). Similarly, on Day 12, the corresponding reductions were 97% and 116%, respectively ($P = 0.022$). At the end of recovery period (Day 24), RGR of *G. lemaneiformis* was still decreased by 58% in the mono-heatwave treatment compared to mono-baseline ($P = 0.013$). GAMM analysis revealed that the negative effects of both mono-heatwave ($P = 0.003$) and co-heatwave ($P < 0.001$) treatments intensified over time, and the inhibitory effect of the co-baseline treatment increased during the heatwave phase and declined during recovery period ($P = 0.003$) (Fig. 2d).

Photosynthetic activity of *H. akashiwo* and *G. lemaneiformis*

Heatwave and coculture treatment significantly affected Fv/Fm and Y(II) of *H. akashiwo*, with coculture mode treatment also showing a significant effect on NPQ on Day 12; by Day 24, only co-culture treatment maintained significant effects on Fv/Fm and Y(II) (Supplementary Table S3). In the coculture system, Fv/Fm was significantly lower compared to the monoculture system on Days 12 ($P < 0.001$) and 24 ($P < 0.001$) (Fig. 3a). Under co-heatwave treatment, Fv/Fm was 58% lower than that under co-baseline treatment on Day 12 ($P < 0.001$). Y(II) was similar tendency with Fv/Fm (Fig. 3c). The co-heatwave treatment showed significantly lower NPQ compared to the mono-control on Day 12 (Fig. 3e, $P = 0.027$). By Day 24, NPQ in all treatments demonstrated no difference (Fig. 3e).

For *G. lemaneiformis*, heatwave had significant effects on Fv/Fm and NPQ on Day 12, and it interacted with coculture treatment on NPQ on Day 24 (Supplementary Table S4). Fv/Fm in heatwave treatment was higher than that in baseline treatment on Day 12 (Fig. 3b, $P = 0.082$). On Day 12, relative to mono-baseline treatment, NPQ increased by 51% and 146% in mono- and co-heatwave treatments, respectively, while it decreased by 48% in co-baseline treatment ($P = 0.024$, Fig. 3f). After recovery period, no significant differences were observed in Fv/Fm or Y(II) among treatments (Fig. 3b, d), whereas NPQ in co-baseline and mono-heatwave treatments remained higher than in the mono-baseline treatment ($P = 0.046$, Fig. 3f).

Photosynthetic pigments of *H. akashiwo* and *G. lemaneiformis*

For *H. akashiwo*, coculture treatment significantly affected on photosynthetic pigments (Chl *a* and carotenoids) on Day 12 (Supplementary Table S3); the mono-heatwave treatment demonstrated the highest contents of Chl *a* ($P = 0.015$) and carotenoids ($P < 0.001$) (Fig. 4a, b). Due to the extremely low cell density of *H. akashiwo* during the recovery period, photosynthetic pigment analysis could not be reliably conducted in the coculture system.

In *G. lemaneiformis*, no significant differences were detected among treatments in Chl *a* or carotenoids during cultivation time (Fig. 4c, d). On Day 12, coculture reduced PE and PC contents, and co-heatwave treatment led to the lowest levels compared to other treatments (Supplementary Table S4, Fig. 4e, f). However, no significant differences were observed in either PE or PC contents among treatments after recovery period (Fig. 4e, f).

The production of hemolytic toxin under heatwave and coculture

Hemolytic activity was notably altered by both heatwave and coculture treatment, with an interaction between these factors on Day 12 (Supplementary Table S3). On Day 6, both coculture and heatwave treatments significantly enhanced hemolytic activity, with the heatwave treatment showing a 21% increase compared to the baseline treatment in the coculture system (Fig. 5a, $P < 0.001$). Following the heatwave period, hemolytic activity in heatwave-treated samples remained elevated across different culture systems. The co-heatwave treatment resulted in the highest hemolytic activity on Day 12 (Fig. 5a, $P < 0.001$). Therefore, when exposed to both heatwave and *G. lemaneiformis*, the hemolytic activity was significantly enhanced (Fig. 5b). GAMM analysis indicated that the positive effect of mono-heatwave treatment diminished over time ($P = 0.025$) (Supplementary Fig. S4). Hemolytic activity

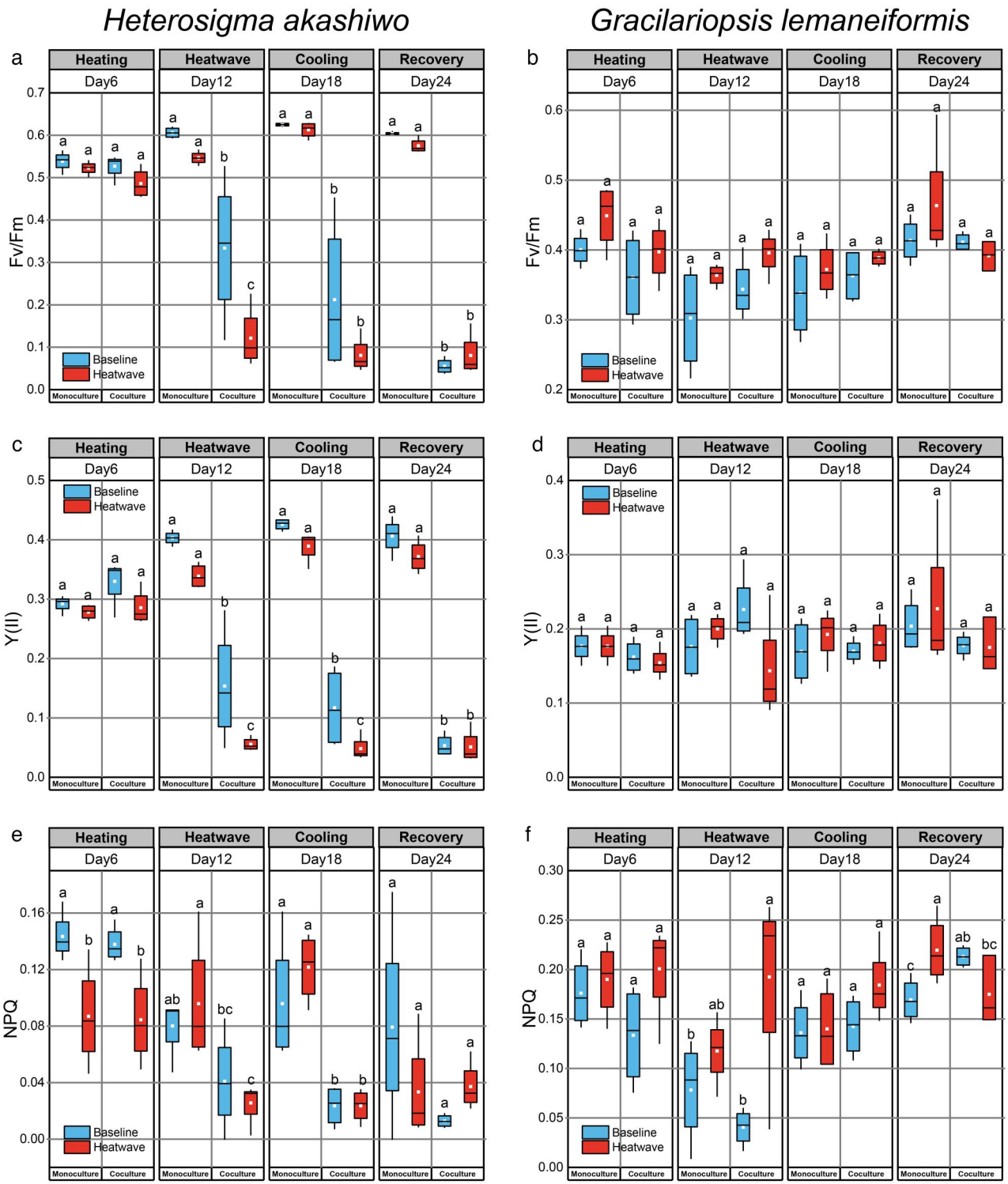

Figure 3: Photosynthetic traits of *H. akashiwo* and *G. lemaneiformis* under different treatments. Maximal photochemical efficiency of PSII (Fv/Fm) of *H. akashiwo* (a) and *G. lemaneiformis* (b); effective quantum yield of PSII (Y(II)) of *H. akashiwo* (c) and *G. lemaneiformis* (d); non-photochemical quenching (NPQ) of *H. akashiwo* (e) and *G. lemaneiformis* (f). Data are presented as boxplots, where white rectangles denote treatment means and whiskers extend to 1.5× the interquartile range. Different letters indicate statistically significant differences among treatments on the same day ($P < 0.05$). Heating, heatwave, cooling and recovery represent the four phases of experiment.

AQ22

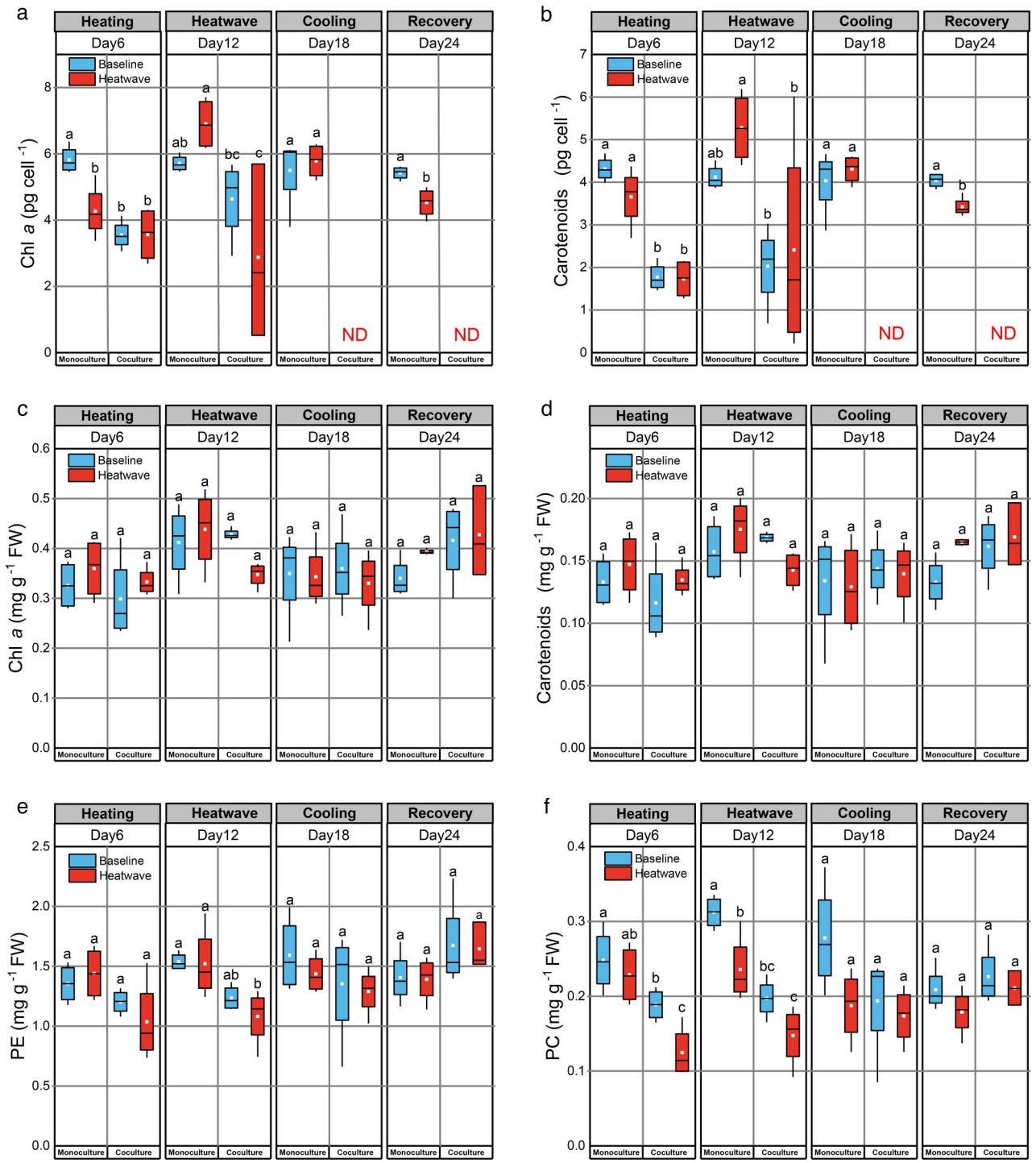

Figure 4: Photosynthetic pigment concentrations of *H. akashiwo* (a–b) and *G. lemaneiformis* (c–f) under different treatments. Data are presented as boxplots, where white rectangles denote treatment means and whiskers extend to 1.5× the interquartile range. 'ND' means no detected, where the cell density of *H. akashiwo* was too low for reliable detection. Different letters indicate statistically significant differences among treatments on the same day ($P < 0.05$). Heating, heatwave, cooling and recovery represent the four phases of experiment.

AQ23

measurements in the cocultures during the recovery period were not conducted due to previously mentioned reason.

Metabolic profile changes of *G. lemaneiformis*

Metabolomic analysis was performed to reveal the mechanisms underlying the effects of coculture

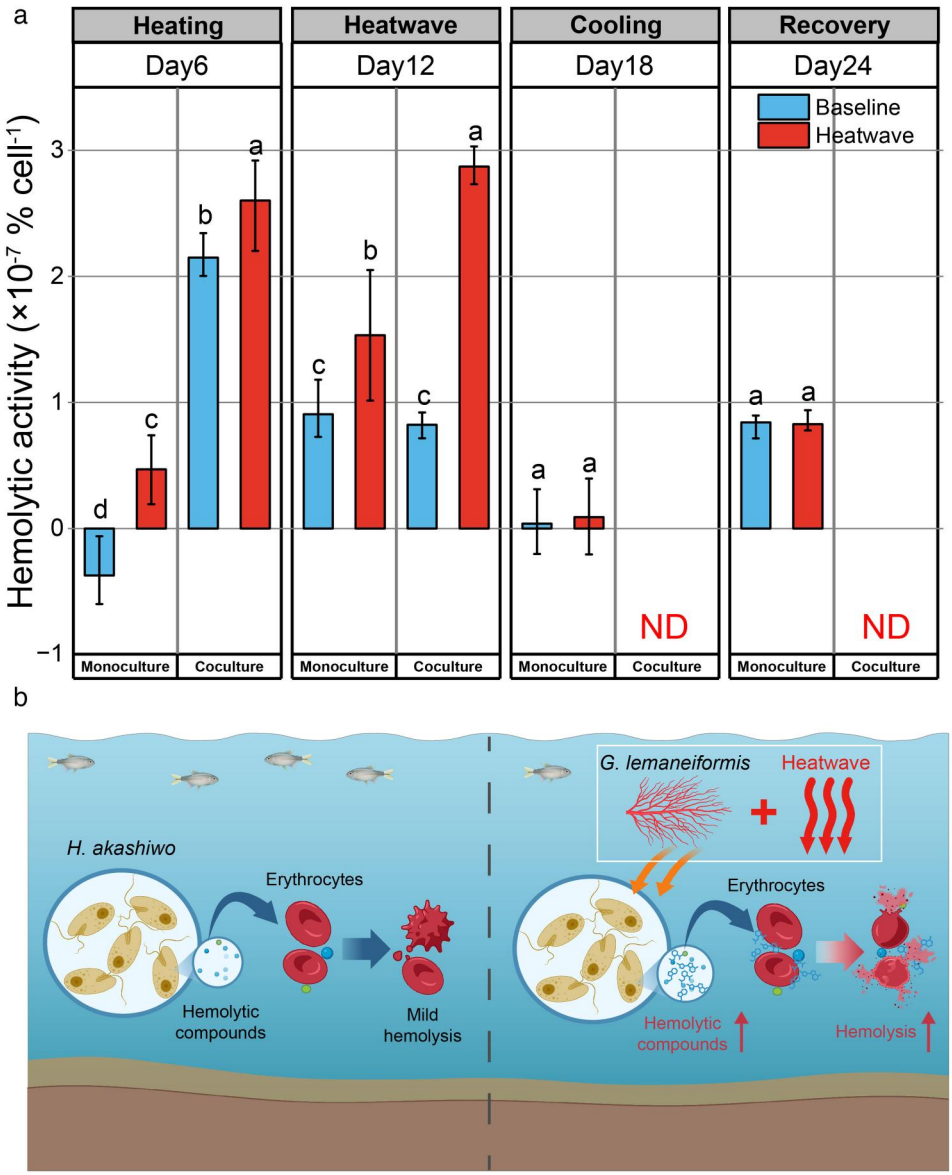

Figure 5: Hemolytic activity of *H. akashiwo* under different treatments. (a) Quantitative analysis of hemolytic activity across treatment groups. Data represent mean ± SD ($n = 3$), with 'ND' indicating samples where activity was not detected due to low cell density of *H. akashiwo*. Different letters denote statistically significant differences between treatments on the same day ($P < 0.05$). Heating, heatwave, cooling and recovery represent the four phases of experiment. (b) Schematic representation of hemolytic activity dynamics in *H. akashiwo* under different experimental conditions: with and without heatwave exposure and *G. lemaneiformis* coculture.

AQ24

and/or heatwave exposure on *G. lemaneiformis*. Partial least squares-discriminant analysis demonstrated clear discrimination among the four treatments in the heatwave period (Day 12) (Fig. 6a), but with considerable overlap observed among treatment groups in the recovery period (Day 24) (Fig. 6b). These results indicate that coculture and/or heatwave significantly altered the metabolic profiles of *G. lemaneiformis* in the heatwave period, while their effects converged in the recovery period.

A total of 1810 metabolites were identified in *G. lemaneiformis*. Compared to mono-baseline, 314, 138 and 258 differentially expressed metabolites (DEMs) were altered under co-baseline, mono-heatwave and co-heatwave treatments during the heatwave period (Supplementary Fig. S5a). In the recovery period, the corresponding DEM counts were 442, 83 and 84, respectively (Supplementary Fig. S5b). KEGG enrichment analysis of these DEMs during the heatwave period (Day 12) identified three pathways

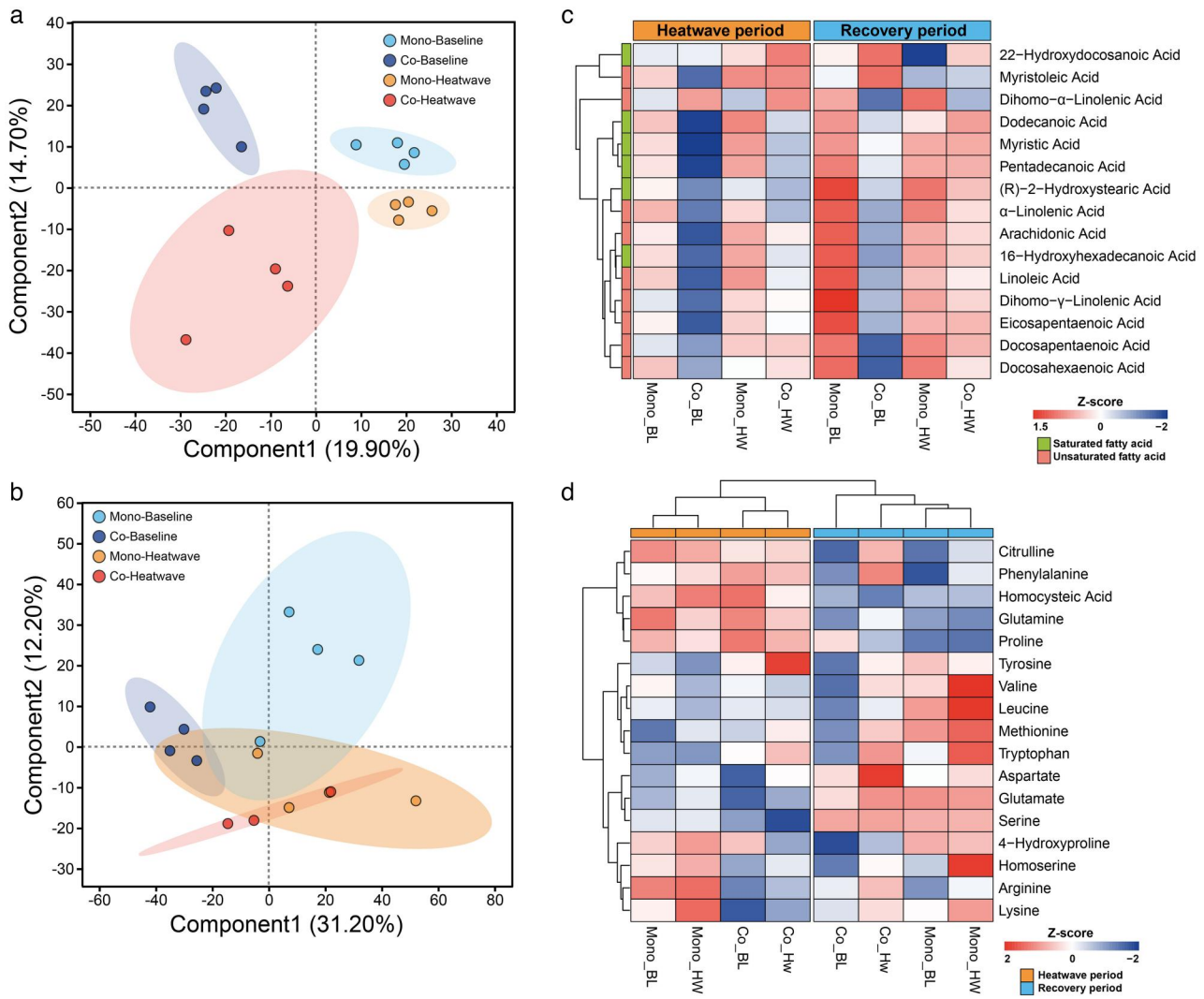

Figure 6: Metabolomics profiling of *G. lemaneiformis* during heatwave (Day 12) and recovery (Day 24) periods. Panels a and b show partial least squares-discriminant analysis of different treatment groups in the heatwave (a) and recovery (b) periods. Panels c and d present the relative abundances and hierarchical clustering for fatty acids (c) and amino acids (d) in *G. lemaneiformis* in heatwave and recovery periods.

AQ25

shared across all treatments: nucleotide metabolism, purine metabolism and ABC transporters (Supplementary Table S5, Supplementary Fig. S6).

Hierarchical clustering analysis was performed on the abundances of fatty acids and amino acids in *G. lemameiformis* across treatments during heatwave and recovery periods (Fig. 6c, d). In contrast to the monoculture treatment, the coculture treatment led to reduce abundances of most fatty acids (e.g. α-linolenic acid, linoleic acid) in *G. lemaneiformis* during the heatwave period (Fig. 6c). Notably, the co-baseline treatment maintained consistently lower fatty acid levels during the recovery period. Most amino acid levels declined during the heatwave period compared to recovery period, except for citrulline, proline, phenylalanine, homocysteic acid and glutamine (Fig. 6d). In the recovery period, fatty acid levels in the co-heatwave treatment showed partial recovery but remained low in the co-baseline treatment. Meanwhile, antioxidant levels gradually restored, though maintaining lower abundances in co-baseline treatment and amino acid profiles demonstrated opposite patterns compared to those observed in the heatwave period.

The metabolic response patterns of *G. lemaneiformis* during heatwave period were illustrated in Fig. 7. Compared to mono-baseline treatment, *G. lemaneiformis* in co-heatwave treatment displayed profound metabolic suppression. This suppression was characterized by significant down-regulation of

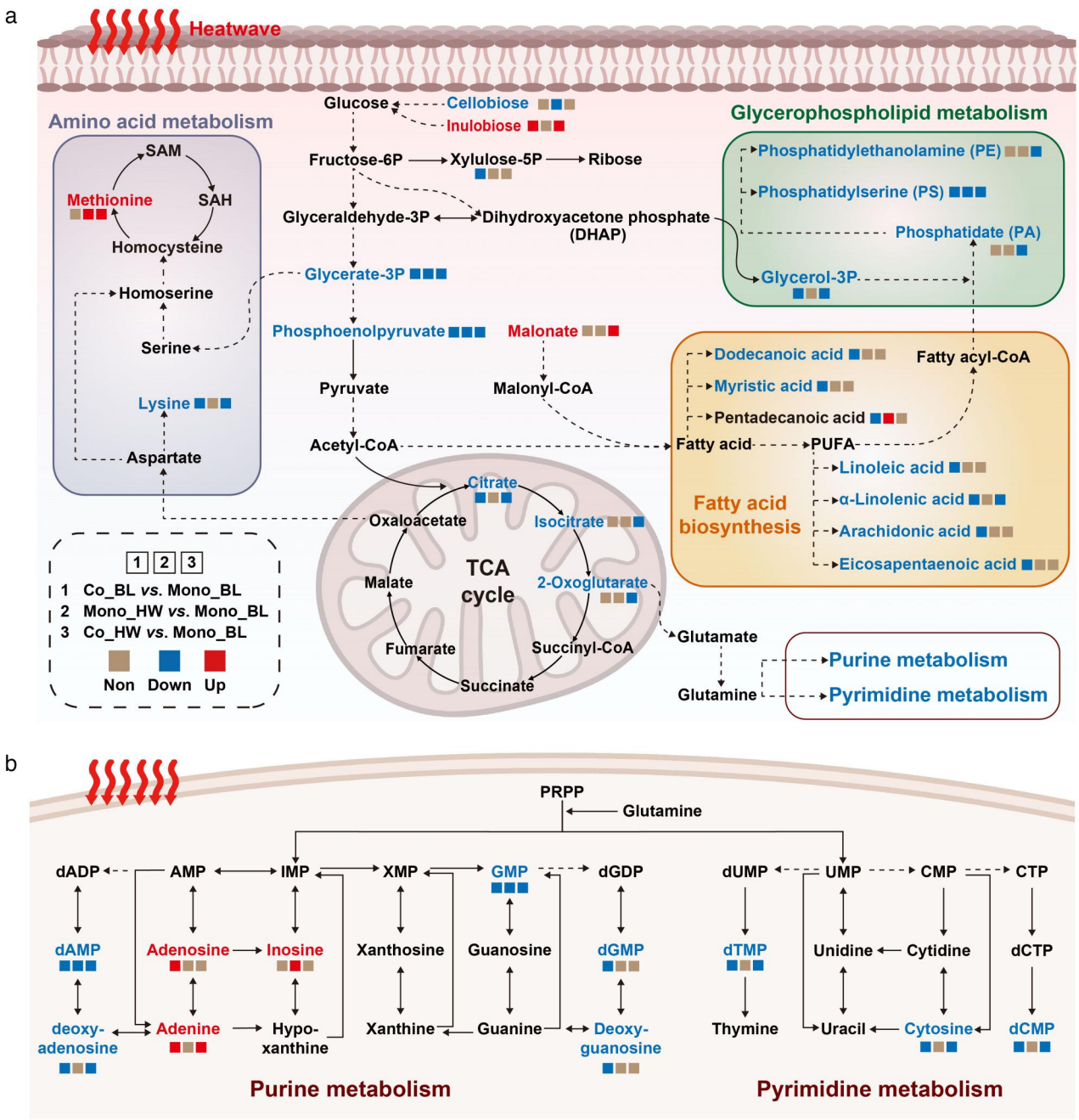

Figure 7: Metabonomic response of *G. lemaneiformis* to *H. akashiwo* during heatwave period (Day 12). Panel a shows the integrated metabolic network analysis revealing key pathways affected by heatwave and *H. akashiwo*. Panel b represents the changes of nucleotide metabolism pathways exposure to heatwave stress. Solid and dotted arrows indicate direct and indirect biochemical interactions. The red and blue rectangles represent significantly upregulated and downregulated metabolites, respectively, while brown rectangles indicate metabolites with no significant changes.

AQ26

key intermediates in both glycolysis (glycerate-3P, phosphoenolpyruvate) and the TCA cycle (citrate, isocitrate, 2-oxoglutarate) (Fig. 7a). Simultaneously, membrane-associated lipids showed marked reduction in the coculture system. This decline encompassed essential fatty acids, including both saturated fatty acids (e.g. dodecanoic acid and myristic acid) and unsaturated fatty acids (e.g. linoleic acid, α-linolenic acid, arachidonic acid, eicosapentaenoic acid), as well as multiple phospholipid classes such as phosphatidate (PA), phosphatidylethanolamine (PE) and phosphatidylserine (PS) (Fig. 7a). Furthermore, nucleotide metabolites (GMP, dAMP, dTMP,

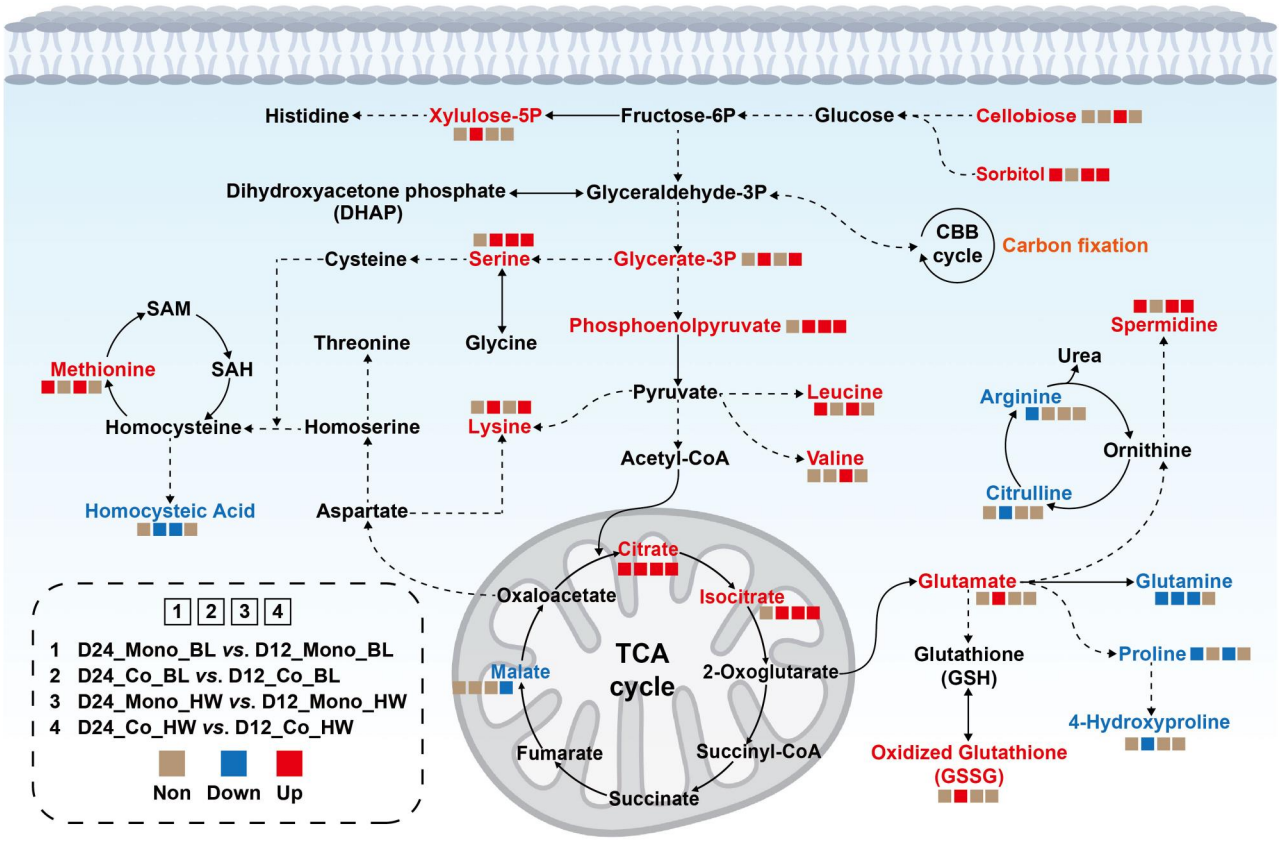

Figure 8: Changes of key metabolic pathways in *G. lemaneiformis* during post-heatwave recovery (Day 24) relative to heatwave period (Day 12). Solid and dotted arrows indicate direct and indirect reactions. The red and blue rectangles indicate significantly upregulated and downregulated metabolites, respectively, while brown rectangles indicate metabolites with no significant change.

AQ27

dCMP, cytosine) exhibited significant down-regulation in the coculture system during the heatwave period (Fig. 7b).

During the recovery period, compared to the heatwave period, the levels of energy metabolism metabolites (glycerate-3P and phosphoenolpyruvate) and amino acids (e.g. lysine, serine, leucine) were significantly elevated. Conversely, glutamine and proline levels decreased (Fig. 8). Concurrently, upregulation of various metabolites associated with nucleotide metabolism were also observed (Supplementary Fig. S8).

DISCUSSION

Physiological responses of *H. akashiwo* to heatwave and *G. lemaneiformis*

The growth of *H. akashiwo* was only marginally affected by the heatwave in monoculture system. This is possibly due to its high adaptability to a wide range of temperatures (18–30 °C), with an optimal growth temperature of 24.11 ± 0.35 °C (Ye *et al.* 2023). The experimental heatwave temperature of 26 °C falls near the optimum growth temperature for *H. akashiwo*. However, when cocultured with *G. lemaneiformis*, *H. akashiwo* suffered pronounced growth suppression that became even more severe under heatwave conditions. The coculture treatment reduced both photosynthetic efficiency (Fig. 3a) and cellular pigment contents, particularly photoprotective carotenoids (Fig. 4b). These changes led to decreased NPQ capacity (Fig. 3e), compromising the cell's ability to scavenge reactive oxygen species (ROS) under stress (Pérez-Gálvez *et al.* 2020; Rezayian *et al.* 2019). In the coculture system, *H. akashiwo* exhibited reduced photoprotective capacity (decreased NPQ and carotenoids) coupled with impaired photosynthetic efficiency (reduced Fv/Fm and Y(II)), which collectively contributed to its growth inhibition. Heatwave exposure further intensified these negative effects. The decline in photosynthetic performance was likely associated with allelopathic

interactions from *G. lemaneiformis*. The α-linolenic acid and linoleic acid have previously been reported as potential allelopathic compounds and were shown to inhibit *H. akashiwo* by triggering mitochondrial apoptosis and impairing its antioxidant and photosynthetic systems (Sun *et al.* 2021; Wang and Liu 2022). In this study, the decreased intracellular abundances of α-linolenic acid and linoleic acid in *G. lemaneiformis* during heatwave period (Supplementary Fig. S5b) suggested they might be released into medium in the coculture system. These compounds could have contributed to the observed suppression of photosynthetic activity in *H. akashiwo*. However, this inference is based on metabolomic results and literature evidence, and direct verification of their release and allelopathic effects in the medium warrants further investigation.

Post-heatwave, *H. akashiwo* in the coculture system maintained a low cell density insufficient for algal blooms. Under stress, *H. akashiwo* can form cysts that remain viable for years (Imai and Itakura 1999), and these can rapidly transform into active planktonic cells when conditions improve (Shikata *et al.* 2007). The observed cell size reduction after the heatwave might be associated with cyst transformation (Supplementary Fig. S9), pending further microscopic evidence of morphological changes. Despite the observed low biomass, monitoring remains essential due to the risk of rapid recovery via potential cyst germination.

Interspecific interactions, particularly competition, can also influence algal toxin production (Cui *et al.* 2024). For instance, when *Microcystis aeruginosa* was co-cultured with *Scenedesmus obliquus*, both intracellular and extracellular microcystin concentrations showed marked increases (Wang *et al.* 2025). Given the high metabolic costs of toxin synthesis, algae typically release only under significant competitive stress (Kearns and Hunter 2000). In our study, the hemolytic compounds (a form of algal toxins) showed higher hemolytic activity in the coculture system on Day 6 compared to monoculture, indicating intense competition between *H. akashiwo* and *G. lemaneiformis* during the early cultivation phase. However, by Day 12, both hemolytic activity and algal growth declined in co-baseline treatment. This suggests that under prolonged competitive stress, *H. akashiwo* prioritizes survival over secondary metabolite production, reallocating energy from hemolytic compound synthesis to essential cellular functions.

Notably, the combined effects of heatwave exposure and co-cultivation with *G. lemaneiformis* significantly enhanced the hemolytic activity of *H. akashiwo* during the heatwave period, with peak levels on both Days 6 and 12, resulting in the highest hemolytic activity among the four treatment groups. This finding warrants attention, since hemolytic activity can exert severe threats on aquaculture and marine ecosystems.

Hemolytic activity of *H. akashiwo* under heatwave and coculture conditions

Our findings revealed that heatwave conditions enhanced the hemolytic activity of *H. akashiwo*, particularly during co-cultivation with *G. lemaneiformis* (Fig. 5b). Environmental factors, such as temperature, light and nutrients, strongly affect production of algal toxins and algal hemolytic activity (Boer *et al.* 2004; Kuroda *et al.* 2005; Vidyarathna *et al.* 2020). Specifically, *H. akashiwo* exhibited peak hemolytic activity at 25 °C compared to 22 °C and 30 °C (Vidyarathna *et al.* 2020). Additionally, previous research has demonstrated that ROS can enhance the effects of hemolytic agents in *Chattonella marina*, a related Raphidophyte species (Marshall *et al.* 2003). Elevated temperatures can increase ROS levels in microalgae (Li *et al.* 2025). This explains the higher hemolytic activity observed in the heatwave treatments compared to the non-heatwave treatments.

Growth responses of *G. lemaneiformis* to heatwave and *H. akashiwo*

Exposure to heatwave stress induced a minor decline in the growth rates of *G. lemaneiformis* under monoculture. The adverse effects of heatwaves intensified over time and persisted through the recovery period. This inhibitory effect was further exacerbated when cocultured with *H. akashiwo*, leading to negative growth rates. These growth variations were closely linked to heatwave and *H. akashiwo* exposure.

High temperatures inhibit the growth rates of *G. lemaneiformis* (Zou and Gao 2014), and, more critically, induce ROS accumulation in *G. lemaneiformis* (Zhang *et al.* 2024), triggering multiple protective mechanisms. The elevated biliverdin levels in heatwave treatments (Supplementary Fig. S7d). Biliverdin maintains chloroplast redox homeostasis through NADPH consumption and serves as a precursor for the antioxidant bilirubin,

thus playing a dual role in oxidative stress defense (Ishikawa *et al.* 2023). Its increase indicated a disruption of chloroplast redox homeostasis in *G. lemaneiformis*. Furthermore, phycobiliproteins demonstrated a notable decrease among treatments during the heatwave period (Day 12) (Fig. 4). This reduction weakened light-harvesting capabilities, which decreases ROS generation at photosynthetic source. This represents an important adaptive mechanism in *G. lemaneiformis*.

Heterosigma akashiwo can secrete allelopathic compounds that inhibit the growth of other algal species (Ji *et al.* 2024; Yamasaki *et al.* 2007). Therefore, the observed growth suppression of *G. lemaneiformis* in this study may be closely related to the allelopathic effects of *H. akashiwo*. The elevated temperatures likely enhance these allelopathic effects (Altman-Kurosaki *et al.* 2025; Ma *et al.* 2015), as higher temperatures often increase the production and potency of inhibitory compounds. Additionally, harmful algal toxins can act as allelopathic compounds with inhibitory effects (Wang *et al.* 2025; Wu *et al.* 2025b). For instance, okadaic acid from *Prorocentrum lima* inhibited *Pyropia yezoensis* growth by disrupting photosynthesis, causing oxidative stress, interfering with nitrogen metabolism and reducing in transcriptional efficiency (Wu *et al.* 2025b). Similarly, the hemolytic compounds from *H. akashiwo* likely act as allelopathic substances, inducing oxidative stress and consequently inhibiting the growth of *G. lemaneiformis*. The present study demonstrated that heatwave conditions significantly increased hemolytic activity, while the observed growth recovery of *G. lemaneiformis* following the decreased hemolytic activity in the co-baseline treatment further supports the inhibitory role of these hemolytic compounds.

After a recovery period at 22 °C, the co-baseline treatment showed normal growth rates comparable to mono-baseline treatment, while heatwave-treated groups demonstrated only minor recovery of growth. *G. lemaneiformis* exhibited distinct physiological and metabolic adjustments under different treatments. In the co-baseline treatment, reduced stress from *H. akashiwo* allowed the macroalga to maintain a stable growth state, which was accompanied by lower abundances of compounds, such as fatty acids and amino acids (Fig. 6c, d). In contrast, physiological performance revealed higher levels of photosynthetic pigments compared to the mono-baseline treatment, indicating elevated photosynthetic potential and energy capture. These changes were supported by metabolic upregulation of key metabolites in glycolysis and the TCA cycle (Fig. 8), as well as increased levels of fatty acids and amino acids, which are essential for energy production and cellular repair processes.

While stable Fv/Fm and phycobiliprotein levels suggested maintenance of photosystem efficiency, higher NPQ demonstrated active photoprotection against oxidative damage. Despite the gradual restoration of photosynthetic function and antioxidant systems, heatwave-treated groups showed persistent negative effects on growth. These can be attributed to a metabolic trade-off, where substantial energy resources were allocated to repairing damaged tissues and maintaining basic metabolic functions, delaying the recovery of growth. As cellular processes continue to normalize, growth recovery is expected to ensue.

Metabolic perturbation of *G. lemaneiformis* and its association with physiological response

Metabolomic analysis revealed metabolic reprogramming in *G. lemaneiformis* under heatwave stress and co-cultivation with *H. akashiwo*. These treatments significantly altered key metabolic pathways, primarily involving carbon, nitrogen, lipid and nucleotide metabolism.

Carbon and nitrogen metabolism

Stress inhibited glycolysis and the TCA cycle, leading to the downregulation of key metabolites, such as glycerate-3-phosphate, phosphoenolpyruvate, citrate and 2-oxoglutarate (Fig. 7a). This restricted the carbon supply and energy production, and ultimately reduced growth in *G. lemaneiformis*. Leucine and valine, which can be catabolized to acetyl-CoA, play a key role in energy metabolism by entering the TCA cycle for energy production (Liang *et al.* 2019). During the heatwave period, the observed reduction in leucine and valine levels suggested increased catabolic activity to meet elevated energy demands during stress, compensating for the suppressed glycolytic and TCA pathways.

Meanwhile, nitrogen metabolism also exhibited compensatory adjustments under stress. Proline accumulation acts as a protective mechanism, providing antioxidative defense and osmotic balance (Matysik *et al.* 2002; Szabados and Savouré 2010). During heatwaves, elevated proline levels were likely critical for enhancing the survival of thalli under adverse conditions (Fig. 6d). Similarly, glutamine, a key intermediate in nitrogen

metabolism, plays essential roles in amino acid synthesis and nitrogen storage. These adaptive changes in C/N metabolism illustrate how macroalgal cells strategically allocate resources toward survival under stress, prioritizing protective mechanisms over growth to endure environmental challenges such as heatwaves.

Lipid metabolism and membrane integrity

The adjustment of fatty acid composition represents a crucial response mechanism in algae adapting to environmental changes (Zhang *et al.* 2020). In this study of *G. lemaneiformis*, co-culture with *H. akashiwo* induced significant alterations in lipid metabolism, characterized by reduced levels of both fatty acids and phospholipids compared to the monoculture system (Fig. 7a). The lower fatty acid contents in co-cultivation treatments might be attributed to increased energy demands under competitive pressure, where fatty acids were converted to acetyl-CoA for energy metabolism. This metabolic shift likely serves as a compensatory mechanism for downregulated TCA cycle metabolites, providing essential energy resources during stress conditions.

Phospholipids are essential components of membranes, maintaining cellular structural integrity (Wang *et al.* 2020). Sustain elevated NPQ is enabled to protect membrane structures under stress (Malnoë *et al.* 2018). Phycobilisomes are anchored to the thylakoid membrane surface (Samsonoff and MacColl 2001). The observed decrease in phospholipids indicated membrane damage. This membrane deterioration induced a protective increase in NPQ, leading to a loss of phycobiliproteins. Consequently, these physiological disruptions led to suppressed growth of *G. lemaneiformis*. Furthermore, the compromised membrane integrity intensified the release of allelopathic substances (particularly α-linolenic acid and linoleic acid), thereby enhancing the growth inhibition of *H. akashiwo*, resulting in mutual growth suppression between macroalgae and microalgae.

Nucleotide metabolism

Alterations in nucleotide metabolism, particularly within the purine and pyrimidine pathways, play a fundamental role in DNA/RNA synthesis and repair (Santos *et al.* 2024). The noticeable change of purine and pyrimidine metabolism pathways across all three treatments during the heatwave period (Fig. 7b), suggests impaired nucleic acid synthesis and repair processes in *G. lemaneiformis* under heatwave stress and *H. akashiwo* co-cultivation. Furthermore, purine metabolism is closely associated with energy metabolism (Liao *et al.* 2025). The upregulation of ATP degradation products (adenine, adenosine and inosine), indicated increased ATP consumption in response to heightened energy demands under pressures. This metabolic shift led to the accumulation of degradation products and ultimately resulted in negative growth of *G. lemaneiformis* during heatwave period.

To summarize, *G. lemaneiformis* exhibited three key metabolic responses under stress: (i) Carbon and nitrogen metabolism showed suppressed glycolysis and the TCA cycle, compensated by amino acids catabolism and proline accumulation for stress protection; (ii) lipid metabolism alterations, characterized by reduced fatty acids and phospholipids, reflected increased energy demands and membrane damage and (iii) nucleotide metabolism disruption, evidenced by ATP degradation product accumulation, indicated impaired cellular repair and elevated energy consumption. These metabolic adaptations collectively demonstrated how *G. lemaneiformis* dynamically allocated resources and prioritized survival mechanisms over growth under environmental stress.

The metabolomic analysis was performed with four biological replicates per treatment. While this sample size is comparable to many previous studies (Liu and Lin 2020; Slaveykova *et al.* 2021; Wu *et al.* 2025a), it is lower than the replicate numbers ($n \geq 6$) often recommended in metabolomics. Therefore, although the major metabolic patterns observed are considered reliable, caution is warranted when interpreting subtle variations, particularly for low-abundance metabolites. In addition, this study focused only on the metabolic responses of *G. lemaneiformis*. Metabolomic profiling of *H. akashiwo* under similar conditions would help provide a more comprehensive understanding of the bidirectional metabolic interactions between the two species and represents an important direction for future research.

Competition of two species under MHWs

MHWs significantly intensified the interspecific competition between *H. akashiwo* and the cultivated macroalga *G. lemaneiformis* by amplifying their bidirectional inhibitory interactions. The differential thermal sensitivity of the two species shapes the

competitive dynamic—*H. akashiwo* shows high tolerance to 26 °C MHW conditions while *G. lemaneiformis* exhibits inherent thermal vulnerability. Heatwaves further enhance the macroalga's allelochemical-mediated suppression of microalgal growth and the microalga's stress-induced hemolytic toxin production, leading to a mutual growth-inhibition pattern where both species reallocate energy from growth to survival-related physiological and metabolic processes. This competitive dynamic has important ecological and practical implications. Ecologically, it reveals the altered interspecific interaction mechanisms of coastal primary producers under climate change-driven extreme thermal stress, and enriches our ecological understanding of how harmful algal bloom-macroalgae symbiotic systems respond to MHWs in coastal aquaculture areas (Zhao *et al.* 2025). In practice, it provides key insights for marine macroalgae aquaculture and HAB ecological control. On one hand, it confirms that *G. lemaneiformis* can still effectively control *H. akashiwo* biomass and prevent HAB outbreaks under MHW conditions, which supports the sustainability of using macroalgae cultivation for HAB mitigation in a warming ocean. On the other hand, it alerts that MHWs will cause severe productivity losses in *G. lemaneiformis* aquaculture, and the elevated hemolytic toxicity of *H. akashiwo* at low biomass poses a hidden ecotoxicological risk to coastal aquaculture ecosystems. Overall, these findings offer critical scientific insights for the adaptive management of economically important macroalgae aquaculture, as well as the comprehensive risk assessment of toxigenic microalgae in coastal waters under future extreme climate scenarios (Seymour and McLellan 2025).

CONCLUSION

This study investigated the growth dynamics and interspecific interactions between *H. akashiwo* and *G. lemaneiformis*, including hemolytic activity under coculture and/or heatwave conditions. The results demonstrated differential thermal sensitivity between species, with *G. lemaneiformis* showing greater vulnerability to heatwave stress compared to *H. akashiwo*. *G. lemaneiformis* exhibited significant inhibitory effects on microalgal growth. Under heatwave conditions, this inhibitory effect was further intensified. Despite experiencing reduced growth rates, *H. akashiwo* maintained elevated hemolytic activity during heatwave exposure, potentially amplifying environmental risks. Meanwhile, interactions with *H. akashiwo* disrupted macroalgal physiological performances (NPQ, phycobiliprotein) and key metabolic processes (C/N, lipid and nucleotide metabolism), ultimately resulting in growth inhibition. Although *G. lemaneiformis* showed signs of metabolic restoration during the post-heatwave period, the sustained negative impact on its growth continued to persist. Notably, even with compromised growth, *G. lemaneiformis* retained sufficient regulatory capacity to maintain *H. akashiwo* populations below harmful levels, demonstrating the robust nature of macroalgal control over harmful algal proliferation. These findings provide novel insights into the interactive relationship between toxic microalgae and commercially vital macroalgae in present day and future extreme weather scenarios. The enhanced inhibitory effects during heatwaves suggest new possibilities for harmful algal bloom management, while greater attention should be paid to the ecotoxicological risks to macroalgae in biological control applications.

Supplementary Material

AQ28

Supplementary material is available at *Journal of Plant Ecology* online.

Text S1: Detailed protocols of hemolytic activity assay.

Text S2: Detailed protocols of metabolomic profiling.

Table S1: Two-way ANOVA analysis of variance for the effects of heatwave and culture on RGR of *H. akashiwo*.

Table S2: Two-way ANOVA analysis of variance for the effects of heatwave and culture on RGR of *G. lemaneiformis*.

Table S3: Two-way ANOVA analysis of variance for the effects of heatwave and culture on Fv/Fm, Y(II), NPQ, Chl *a*, carotenoids and hemolytic activity of *H. akashiwo*.

Table S4: Two-way ANOVA analysis of variance for the effects of heatwave and culture on Fv/Fm, Y(II), NPQ, Chl *a*, carotenoids, PE and PC of *G. lemaneiformis*.

Table S5: The key pathways compared to the mono-baseline treatment in the co-baseline, mono-heatwave and co-heatwave treatments in the heatwave period ($P < 0.05$).

Figure S1: The effects of antibiotic treatment on *H. akashiwo*.

Figure S2: The physiological performances on *G. lemaneiformis* in preliminary experiments.
Figure S3: The nutrient levels in the different culture system of *H. akashiwo* and *G. lemaneiformis* during the experimental time.
Figure S4: GAMM analysis of the hemolytic activity of *H. akashiwo* under mono-heatwave treatment.
Figure S5: Analysis of differential metabolites in *G. lemaneiformis*.
Figure S6: KEGG enrichment analysis among different treatments in the heatwave period (Day 12).
Figure S7: Box plots of the abundance of metabolites with significant alterations among all treatments during heatwave period (Day 12).
Figure S8: The changes of nucleotide metabolism pathways during post-heatwave recovery (Day 24).
Figure S9: The changes of cell size in *H. akashiwo* under different conditions during the experiment.

Author contributions

Yonglong Xiong (Data curation, Formal analysis, Investigation, Methodology, Software, Writing—original draft), Jingke Ge (Data curation, Formal analysis, Investigation, Methodology, Software), Fei-Xue Fu (Formal analysis, Methodology, Validation, Writing—review & editing), David A Hutchins (Formal analysis, Methodology, Validation, Writing—review & editing), Lixue Luo (Investigation, Methodology), Jiaying Wen (Investigation, Methodology), and Guang Gao (Conceptualization, Data curation, Formal analysis, Funding acquisition, Investigation, Methodology, Project administration, Resources, Software, Supervision, Validation, Visualization, Writing—original draft, Writing—review & editing)

Funding

This work was supported by the International Cooperation Seed Funding Project for China's Ocean Decade Actions (GHZZ3702840002024020000020), the Open Foundation of Key Laboratory of Marine Environmental Survey Technology and Application, Ministry of Natural Resources (MESTA-2024-A001), the Natural Science Foundation of Xiamen, China (3502Z202572002) and Ocean Negative Carbon Emissions (ONCE) program, and by USC Sea Grant funding to D.A.H. and F.X.F.

Acknowledgements

The authors were grateful to the laboratory technicians Wenyan Zhao and Xianglan Zeng and to Di Zhang and Weijia Chen for their help with data processing.

Conflict of interest statement. The authors declare that they have no conflict of interest.

REFERENCES

Accoroni S, Percopo I, Cerino F, *et al.* (2015) Allelopathic interactions between the HAB dinoflagellate *Ostreopsis* cf. *ovata* and macroalgae. *Harmful Algae* **49**:147–155. https://doi.org/10.1016/j.hal.2015.08.007

Altman-Kurosaki NT, Pratte ZA, Stewart FJ, *et al.* (2025) Coral–algal competition: allelopathy, temporal variance, and effects on coral microbiomes. *Coral Reefs (Online)* **44**:49–62. https://doi.org/10.1007/s00338-024-02585-7

Bao B, Ren G (2014) Climatological characteristics and long-term change of SST over the marginal seas of China. *Continental Shelf Research* **77**:96–106. https://doi.org/10.1016/j.csr.2014.01.013

Baohong C, Kang W, Xu D, *et al.* (2021) Long-term changes in red tide outbreaks in Xiamen Bay in China from 1986 to 2017. *Estuarine, Coastal and Shelf Science* **249**:107095. https://doi.org/10.1016/j.ecss.2020.107095

Beer S, Eshel A (1985) Determining phycoerythrin and phycocyanin concentrations in aqueous crude extracts of red algae. *Australian Journal of Marine and Freshwater Research* **36**:785–792. https://doi.org/10.1071/MF9850785

Boer MK, Tyl MR, Vrieling EG, *et al.* (2004) Effects of salinity and nutrient conditions on growth and haemolytic activity of *Fibrocapsa japonica* (Raphidophyceae). *Aquatic Microbial Ecology* **37**:171–181. https://doi.org/10.3354/ame037171

Bulleri F, Pedicini L, Bertocci I, *et al.* (2025) The impact of a marine heatwave on the productivity and carbon budget of a NW Mediterranean seaweed forest. *Marine Pollution Bulletin* **212**:117595. https://doi.org/10.1016/j.marpolbul.2025.117595

Chai Z, Hu Z, Deng Y, *et al.* (2021) Interactions between the seaweed *Gracilaria* and dinoflagellate *Akashiwo sanguinea* in an indoor co-cultivation system and the interference of bacteria. *Journal of Applied Phycology* **33**:3153–3163. https://doi.org/10.1007/s10811-021-02532-x

Chai ZY, He ZL, Deng YY, *et al.* (2018) Cultivation of seaweed *Gracilaria lemaneiformis* enhanced biodiversity in a eukaryotic plankton community as revealed via metagenomic analyses. *Molecular Ecology* **27**:1081–1093. https://doi.org/10.1111/mec.14496

Cheng X, Zhao X, Lin J, *et al.* (2024) Rotation culture of macroalgae based on photosynthetic physiological characteristics of algae. *Biology* **13**:459. https://doi.org/10.3390/biology13060459

Cui X, Yang N, Cui H, *et al.* (2024) Interspecific competition enhances microcystin production by *Microcystis aeruginosa* under the interactive influences of temperature and nutrients. *Water Research* **265**:122308. https://doi.org/10.1016/j.watres.2024.122308

Dai Y, Yang S, Zhao D, *et al.* (2023) Coastal phytoplankton blooms expand and intensify in the 21st century. *Nature* **615**:280–284. https://doi.org/10.1038/s41586-023-05760-y

Eschbach E, Scharsack JP, John U, *et al.* (2001) Improved erythrocyte lysis assay in microtitre plates for sensitive detection and efficient measurement of haemolytic compounds from ichthyotoxic algae. *Journal of Applied Toxicology* **21**:513–519. https://doi.org/10.1002/jat.797

Fei X (2004) Solving the coastal eutrophication problem by large scale seaweed cultivation. *Hydrobiologia* **512**:145–151. https://doi.org/10.1023/B:HYDR.0000020320.68331.ce

Frölicher TL, Laufkötter C (2018) Emerging risks from marine heat waves. *Nature Communications* **9**:650. https://doi.org/10.1038/s41467-018-03163-6

Fu F-X, Zhang Y, Warner ME, *et al.* (2008) A comparison of future increased CO_2 and temperature effects on sympatric *Heterosigma akashiwo* and *Prorocentrum minimum*. *Harmful Algae* **7**:76–90. https://doi.org/10.1016/j.hal.2007.05.006

Gao G, Fu Q, Beardall J, *et al.* (2019) Combination of ocean acidification and warming enhances the competitive advantage of *Skeletonema costatum* over a green tide alga, *Ulva linza*. *Harmful Algae* **85**:101698. https://doi.org/10.1016/j.hal.2019.101698

Gao G, Gao L, Jiang M, *et al.* (2022) The potential of seaweed cultivation to achieve carbon neutrality and mitigate deoxygenation and eutrophication. *Environmental Research Letters* **17**:014018. https://doi.org/10.1088/1748-9326/ac3fd9

Gao L, Xiong Y, Fu F-X, *et al.* (2024) Marine heatwaves alter competition between the cultured macroalga *Gracilariopsis lemaneiformis* and the harmful bloom alga *Skeletonema costatum*. *The Science of the Total Environment* **947**:174345. https://doi.org/10.1016/j.scitotenv.2024.174345

García-Poza S, Pacheco D, Cotas J, *et al.* (2022) Marine macroalgae as a feasible and complete resource to address and promote Sustainable Development Goals (SDGs). *Integrated Environmental Assessment and Management* **18**:1148–1161. https://doi.org/10.1002/ieam.4598

Hallegraeff G, Enevoldsen H, Zingone A (2021) Global harmful algal bloom status reporting. *Harmful Algae* **102**:101992. https://doi.org/10.1016/j.hal.2021.101992

Hayashida H, Matear RJ, Strutton PG (2020) Background nutrient concentration determines phytoplankton bloom response to marine heatwaves. *Global Change Biology* **26**:4800–4811. https://doi.org/10.1111/gcb.15255

Hobday AJ, Alexander LV, Perkins SE, *et al.* (2016) A hierarchical approach to defining marine heatwaves. *Progress in Oceanography* **141**:227–238. https://doi.org/10.1016/j.pocean.2015.12.014

Hu Z, Liu Q, Zheng L, *et al.* (2026) Nitrate limitation resulting from red tide blooms as a key factor of biomass loss in cultivated kelp *Saccharina japonica*. *Aquaculture* **614**:743580. https://doi.org/10.1016/j.aquaculture.2025.743580

Imai I, Itakura S (1999) Importance of cysts in the population dynamics of the red tide flagellate *Heterosigma akashiwo* (Raphidophyceae). *Marine Biology* **133**:755–762. https://doi.org/10.1007/s002270050517

Ishikawa K, Xie X, Osaki Y, *et al.* (2023) Bilirubin is produced nonenzymatically in plants to maintain chloroplast redox status. *Science Advances* **9**:eadh4787. https://doi.org/10.1126/sciadv.adh4787

Ji N, Chen Y, Xu M, *et al.* (2024) The allelopathic effects of *Heterosigma akashiwo* on *Skeletonema costatum*: insights from gene expression and metabolomics analysis. *The Science of the Total Environment* **945**:173913. https://doi.org/10.1016/j.scitotenv.2024.173913

Ji N, Lin L, Li L, *et al.* (2018) Metatranscriptome analysis reveals environmental and diel regulation of a *Heterosigma akashiwo* (raphidophyceae) bloom. *Environmental Microbiology* **20**:1078–1094. https://doi.org/10.1111/1462-2920.14045

Jiang M, Gao L, Huang R, *et al.* (2022) Differential responses of bloom-forming *Ulva intestinalis* and economically important *Gracilariopsis lemaneiformis* to marine heatwaves under changing nitrate conditions. *The Science of the Total Environment* **840**:156591. https://doi.org/10.1016/j.scitotenv.2022.156591

Kearns KD, Hunter MD (2000) Green algal extracellular products regulate antialgal toxin production in a cyanobacterium. *Environmental Microbiology* **2**:291–297. https://doi.org/10.1046/j.1462-2920.2000.00104.x

Kuroda A, Nakashima T, Yamaguchi K, *et al.* (2005) Isolation and characterization of light-dependent hemolytic cytotoxin from harmful red tide phytoplankton *Chattonella marina*. *Comparative Biochemistry and Physiology: Part C, Pharmacology, Toxicology & Endocrinology* **141**:297–305. https://doi.org/10.1016/j.cca.2005.07.009

Laufkötter C, Zscheischler J, Frölicher TL (2020) High-impact marine heatwaves attributable to human-induced global warming. *Science* **369**:1621–1625. https://doi.org/10.1126/science.aba0690

Li H, Zhang Z, Xiong T, *et al.* (2022) Carbon sequestration in the form of recalcitrant dissolved organic carbon in a seaweed (kelp) farming environment. *Environmental Science & Technology* **56**:9112–9122. https://doi.org/10.1021/acs.est.2c01535

Li J, Ruan Y, Mak YL, *et al.* (2021) Occurrence and trophodynamics of marine lipophilic phycotoxins in a subtropical marine food web. *Environmental Science & Technology* **55**:8829–8838. https://doi.org/10.1021/acs.est.1c01812

Li L, Huang W, Qiao D, *et al.* (2025) Marine heatwaves exacerbate the toxic effects of tire particle leachate on microalgae. *Environmental Science & Technology* **59**:177–187. https://doi.org/10.1021/acs.est.4c08986

Li X (2021) Occurrence characteristics of the red tide in Fujian coastal waters during the last two decades (in Chinese). *Marine Environmental Science* **40**:601–610. https://doi.org/10.12111/j.mes.20200120

Li Y, Ren G, Wang Q, *et al.* (2019) More extreme marine heatwaves in the China Seas during the global warming hiatus. *Environmental Research Letters* **14**:104010. https://doi.org/10.1088/1748-9326/ab28bc

Liang Y, Kong F, Torres-Romero I, *et al.* (2019) Branched-chain amino acid catabolism impacts triacylglycerol homeostasis in *Chlamydomonas reinhardtii*. *Plant Physiology* **179**:1502–1514. https://doi.org/10.1104/pp.18.01584

Liao J, Lu Y, Liu Y, *et al.* (2025) How heatwaves impact microalgae in the presence of environmentally relevant PFAS concentration: metabolic shifts and challenges

posed. *Journal of Hazardous Materials* **484**:136640. https://doi.org/10.1016/j.jhazmat.2024.136640

Lim YK, Park BS, Kim JH, *et al.* (2021) Effect of marine heatwaves on bloom formation of the harmful dinoflagellate *Cochlodinium polykrikoides*: two sides of the same coin? *Harmful Algae* **104**:102029. https://doi.org/10.1016/j.hal.2021.102029

Ling C, Trick CG (2010) Expression and standardized measurement of hemolytic activity in *Heterosigma akashiwo*. *Harmful Algae* **9**:522–529. https://doi.org/10.1016/j.hal.2010.04.004

Liu L, Lin L (2020) Effect of heat stress on *Sargassum fusiforme* leaf metabolome. *Journal of Plant Biology* **63**:229–241. https://doi.org/10.1007/s12374-020-09247-5

Ma Z, Fang T, Thring RW, *et al.* (2015) Toxic and non-toxic strains of *Microcystis aeruginosa* induce temperature dependent allelopathy toward growth and photosynthesis of *Chlorella vulgaris*. *Harmful Algae* **48**:21–29. https://doi.org/10.1016/j.hal.2015.07.002

Malnoë A, Schultink A, Shahrasbi S, *et al.* (2018) The plastid lipocalin LCNP is required for sustained photoprotective energy dissipation in Arabidopsis. *The Plant Cell* **30**:196–208. https://doi.org/10.1105/tpc.17.00536

Mardones JI, Paredes-Mella J, Flores-Leñero A, *et al.* (2023) Extreme harmful algal blooms, climate change, and potential risk of eutrophication in Patagonian fjords: insights from an exceptional *Heterosigma akashiwo* fish-killing event. *Progress in Oceanography* **210**:102921. https://doi.org/10.1016/j.pocean.2022.102921

Marshall J-A, Nichols PD, Hamilton B, *et al.* (2003) Ichthyotoxicity of *Chattonella marina* (Raphidophyceae) to damselfish (*Acanthochromis polycanthus*): the synergistic role of reactive oxygen species and free fatty acids. *Harmful Algae* **2**:273–281. https://doi.org/10.1016/S1568-9883(03)00046-5

Matysik J, Alia, Bhalu B, *et al.* (2002) Molecular mechanisms of quenching of reactive oxygen species by proline under stress in plants. *Current Science* **82**:525–532.

McCabe RM, Hickey BM, Kudela RM, *et al.* (2016) An unprecedented coastwide toxic algal bloom linked to anomalous ocean conditions. *Geophysical Research Letters* **43**:366–310, 376. https://doi.org/10.1002/2016GL070023

McPherson ML, Finger DJ, Houskeeper HF, *et al.* (2021) Large-scale shift in the structure of a kelp forest ecosystem co-occurs with an epizootic and marine heatwave. *Communications Biology* **4**:298. https://doi.org/10.1038/s42003-021-01827-6

O'Boyle S, McDermott G, Silke J, *et al.* (2016) Potential impact of an exceptional bloom of *Karenia mikimotoi* on dissolved oxygen levels in waters off Western Ireland. *Harmful Algae* **53**:77–85. https://doi.org/10.1016/j.hal.2015.11.014

Oliver ECJ, Donat MG, Burrows MT, *et al.* (2018) Longer and more frequent marine heatwaves over the past century. *Nature Communications* **9**:1324. https://doi.org/10.1038/s41467-018-03732-9

Pérez-Gálvez A, Viera I, Roca M (2020) Carotenoids and chlorophylls as antioxidants. *Antioxidants* **9**:505. https://doi.org/10.3390/antiox9060505

Pflugmacher S, Olin M, Kankaanpää H (2010) Oxidative stress response in the red alga *Furcellaria lumbricalis* (Huds.) Lamour. due to exposure and uptake of the cyanobacterial toxin nodularin from *Nodularia spumigena*. *Harmful Algae* **10**:49–55. https://doi.org/10.1016/j.hal.2010.06.004

Porra RJ, Thompson WA, Kriedemann PE (1989) Determination of accurate extinction coefficients and simultaneous equations for assaying chlorophylls a and b extracted with four different solvents: verification of the concentration of chlorophyll standards by atomic absorption spectroscopy. *Biochimica Et Biophysica Acta* **975**:384–394. https://doi.org/10.1016/S0005-2728(89)80347-0

Rezayian M, Niknam V, Ebrahimzadeh H (2019) Oxidative damage and antioxidative system in algae. *Toxicology Reports* **6**:1309–1313. https://doi.org/10.1016/j.toxrep.2019.10.001

Roberts SD, Van Ruth PD, Wilkinson C, *et al.* (2019) Marine heatwave, harmful algae blooms and an extensive fish kill event during 2013 in South Australia. *Frontiers in Marine Science* **6**:610. https://doi.org/10.3389/fmars.2019.00610

Samsonoff WA, MacColl R (2001) Biliproteins and phycobilisomes from cyanobacteria and red algae at the extremes of habitat. *Archives of Microbiology* **176**:400–405. https://doi.org/10.1007/s002030100346

Santos JP, Li W, Keller AA, *et al.* (2024) Mercury species induce metabolic reprogramming in freshwater diatom *Cyclotella meneghiniana*. *Journal of Hazardous Materials* **465**:133245. https://doi.org/10.1016/j.jhazmat.2023.133245

Seymour JR, McLellan SL (2025) Climate change will amplify the impacts of harmful microorganisms in aquatic ecosystems. *Nature Microbiology* **10**:615–626. https://doi.org/10.1038/s41564-025-01948-2

Sheng X, Zuo X, Luo L, *et al.* (2025) Impact of carbon and nitrogen assimilation in *Sargassum fusiforme* (Harvey) setchell due to marine heatwave under global warming. *Global Change Biology* **31**:e70074. https://doi.org/10.1111/gcb.70074

Shikata T, Nagasoe S, Matsubara T, *et al.* (2007) Effects of temperature and light on cyst germination and germinated cell survival of the noxious raphidophyte *Heterosigma akashiwo*. *Harmful Algae* **6**:700–706. https://doi.org/10.1016/j.hal.2007.02.008

Slaveykova VI, Majumdar S, Regier N, *et al.* (2021) Metabolomic responses of green alga *Chlamydomonas reinhardtii* exposed to sublethal concentrations of inorganic and methylmercury. *Environmental Science & Technology* **55**:3876–3887. https://doi.org/10.1021/acs.est.0c08416

Strickland JDH, Parsons TR (1972) A practical handbook of seawater analysis.

Sun S, Hu S, Zhang B, *et al.* (2021) Allelopathic effects and potential allelochemical of *Sargassum fusiforme* on red tide microalgae *Heterosigma akashiwo*. *Marine Pollution Bulletin* **170**:112673. https://doi.org/10.1016/j.marpolbul.2021.112673

Sylvers LH, Gobler CJ (2021) Mitigation of harmful algal blooms caused by *Alexandrium catenella* and reduction in saxitoxin accumulation in bivalves using cultivable

seaweeds. *Harmful Algae* **105**:102056. https://doi.org/10.1016/j.hal.2021.102056

Szabados L, Savouré A (2010) Proline: a multifunctional amino acid. *Trends in Plant Science* **15**:89–97. https://doi.org/10.1016/j.tplants.2009.11.009

Vidyarathna NK, Papke E, Coyne KJ, *et al.* (2020) Functional trait thermal acclimation differs across three species of mid-Atlantic harmful algae. *Harmful Algae* **94**:101804. https://doi.org/10.1016/j.hal.2020.101804

Wang Q, Li X, Yan T, *et al.* (2021) Laboratory simulation of dissolved oxygen reduction and ammonia nitrogen generation in the decay stage of harmful algae bloom. *Journal of Oceanology and Limnology* **39**:500–507. https://doi.org/10.1007/s00343-020-9295-2

Wang R, Liu Q (2022) Responses of bloom-forming *Heterosigma akashiwo* to allelochemical linoleic acid: growth inhibition, oxidative stress and apoptosis. *Frontiers in Marine Science* **8**:793567. https://doi.org/10.3389/fmars.2021.793567

Wang Y, Zhang X, Huang G, *et al.* (2020) Dynamic changes in membrane lipid composition of leaves of winter wheat seedlings in response to PEG-induced water stress. *BMC Plant Biology* **20**:84. https://doi.org/10.1186/s12870-020-2257-1

Wang Z, Yu S, Nie Y, *et al.* (2025) Effects of acetochlor on the interaction between *Scenedesmus* and *Microcystis*: integrated perspectives on toxicity, biotransformation, and competition strategies. *Journal of Hazardous Materials* **481**:136470. https://doi.org/10.1016/j.jhazmat.2024.136470

Wu F, Zhang H, Beardall J, *et al.* (2025a) Metabolite-Mediated trophic interactions: long-term responses of *Thalassiosira weissflogi*i to high CO_2 and warming have cascading effects on consumer metabolism. *Global Change Biology* **31**:e70343. https://doi.org/10.1111/gcb.70343

Wu R, Qiu J, Tang X, *et al.* (2025b) Effects of okadaic acid on *Pyropia yezoensis*: evidence from growth, photosynthesis, oxidative stress and transcriptome analysis. *Journal of Hazardous Materials* **491**:137902. https://doi.org/10.1016/j.jhazmat.2025.137902

Xiong Y, Gao L, Qu L, *et al.* (2023) The contribution of fish and seaweed mariculture to the coastal fluxes of biogenic elements in two important aquaculture areas, China. *The Science of the Total Environment* **856**:159056. https://doi.org/10.1016/j.scitotenv.2022.159056

Yamasaki Y, Nagasoe S, Matsubara T, *et al.* (2007) Allelopathic interactions between the bacillariophyte *Skeletonema costatum* and the raphidophyte *Heterosigma akashiwo*. *Marine Ecology Progress Series* **339**:83–92. https://doi.org/10.3354/meps339083

Ye M, Xiao M, Zhang S, *et al.* (2023) Multi-trait analysis reveals large interspecific differences for phytoplankton in response to thermal change. *Marine Environmental Research* **188**:106008. https://doi.org/10.1016/j.marenvres.2023.106008

Zhang D, Sun J-Z, Fu M-H, *et al.* (2024) Photosynthetic performance and antioxidant activity of *Gracilariopsis lemaneiformis* are sensitive to phosphorus deficiency in elevated temperatures. *Frontiers in Marine Science* **11**:1432937. https://doi.org/10.3389/fmars.2024.1432937

Zhang X, Wu C, Hu C, *et al.* (2020) Lipid remodeling associated with chitooligosaccharides-induced heat tolerance of marine macroalgae *Gracilariopsis lemaneiformis*. *Algal Research* **52**:102113. https://doi.org/10.1016/j.algal.2020.102113

Zhao X, Gao L, Li X, *et al.* (2025) Differential responses of an economically important macroalga and a bloom-forming microalga to marine heatwaves in a coculture system. *Aquaculture* **599**:742111. https://doi.org/10.1016/j.aquaculture.2024.742111

Zhu Z, Qu P, Fu F, *et al.* (2017) Understanding the blob bloom: warming increases toxicity and abundance of the harmful bloom diatom *Pseudo-nitzschia* in California coastal waters. *Harmful Algae* **67**:36–43. https://doi.org/10.1016/j.hal.2017.06.004

Zou D, Gao K (2014) Temperature response of photosynthetic light- and carbon-use characteristics in the red seaweed *Gracilariopsis lemaneiformis* (Gracilariales, Rhodophyta). *Journal of Phycology* **50**:366–375. https://doi.org/10.1111/jpy.12171